ILAR Journal, 2020, Vol. 61, No. 2–3, 274–285

https://doi.org/10.1093/ilar/ilaa029
Review

Magnetic Resonance Imaging of Marmoset Monkeys

David J. Schaeffer[1], CiRong Liu[2], Afonso C. Silva[1] and Stefan Everling[3]

[1]Department of Neurobiology, University of Pittsburgh, Pittsburgh, Pennsylvania, USA, [2]Institute of Neuroscience, Center for Excellence in Brain Science and Intelligence Technology, Chinese Academy of Sciences, Shanghai, China and [3]Department of Physiology and Pharmacology, Robarts Research Institute, University of Western Ontario, London, Ontario, Canada

*__Corresponding Author:__ Stefan Everling, PhD, Centre for Functional and Metabolic Mapping, Robarts Research Institute, 1151 Richmond Street North, London, Ontario N6A 5B7. E-mail: severlin@uwo.ca.

Abstract

The use of the common marmoset monkey (*Callithrix jacchus*) for neuroscientific research has grown markedly in the last decade. Magnetic resonance imaging (MRI) has played a significant role in establishing the extent of comparability of marmoset brain architecture with the human brain and brains of other preclinical species (eg, macaques and rodents). As a non-invasive technique, MRI allows for the flexible acquisition of the same sequences across different species in vivo, including imaging of whole-brain functional topologies not possible with more invasive techniques. Being one of the smallest New World primates, the marmoset may be an ideal nonhuman primate species to study with MRI. As primates, marmosets have an elaborated frontal cortex with features analogous to the human brain, while also having a small enough body size to fit into powerful small-bore MRI systems typically employed for rodent imaging; these systems offer superior signal strength and resolution. Further, marmosets have a rich behavioral repertoire uniquely paired with a lissencephalic cortex (like rodents). This smooth cortical surface lends itself well to MRI and also other invasive methodologies. With the advent of transgenic modification techniques, marmosets have gained significant traction as a powerful complement to canonical mammalian modelling species. Marmosets are poised to make major contributions to preclinical investigations of the pathophysiology of human brain disorders as well as more basic mechanistic explorations of the brain. The goal of this article is to provide an overview of the practical aspects of implementing MRI and fMRI in marmosets (both under anesthesia and fully awake) and discuss the development of resources recently made available for marmoset imaging.

Key words: marmoset, magnetic resonance imaging, awake fMRI, anesthesia

INTRODUCTION

Magnetic resonance imaging (MRI) of laboratory animals has increased precipitously over the past 2 decades (Figure 1). Owing in part to the flexibility to acquire the same sequences across different species in vivo, MRI has been fundamentally important for providing translationally relevant insights in the neurosciences. Initially, laboratory animals were important for developing the MRI technique itself[1,2] but have since been informative for preclinical and neuroscientific investigations.[3] Given their phylogenetic proximity to humans,[4] nonhuman primates (NHP) have been central to this effort, allowing for comparisons of whole-brain structural and functional connectomics, often corroborated by more invasive gold-standard anatomical tracing techniques.[3,5–10] Further, studies of task-based behavior, invasive electrophysiological recording and neuromodulation, and pharmacological challenge have allowed for significant connections to be made across the translational gap.[11–18] While parallel insights have been made in rodents,[19–21] these smaller

Received: April 21, 2020. **Revised:** September 22, 2020. **Accepted:** October 23, 2020

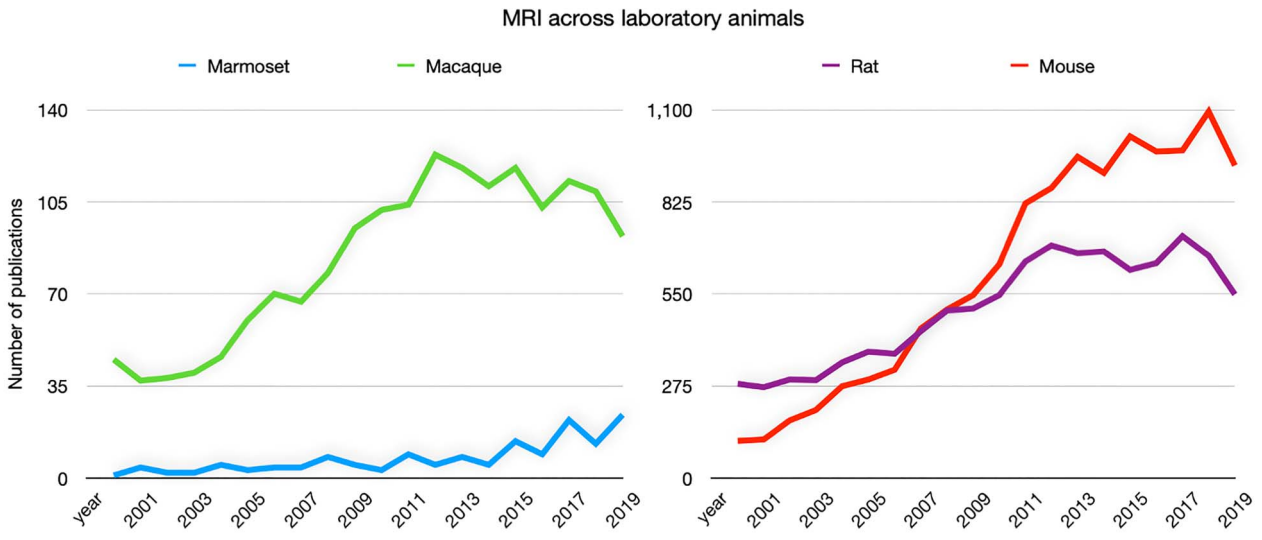

Figure 1: Number of annual publications for marmosets, macaques, rats, and mice related to MRI since the year 2000. Data obtained by searching the respective species name and "magnetic resonance imaging" via PubMed (https://pubmed.ncbi.nlm.nih.gov/).

species have also benefited from the development of specialized ultra-high field strength small-animal MRI systems that offer exquisite spatial resolution and signal strength in vivo.

As one of the smallest New World primates, the common marmoset (*Callithrix jacchus*) may be an ideal NHP species to study with MRI. As primates, marmosets have an elaborated frontal cortex with features analogous to the human brain while also having a small enough body size to fit into powerful small-bore MRI systems.[22,23] Practically, the small size of the marmoset also aides in the ease of handling for MRI studies, a major advantage for imaging marmosets over larger NHP species (eg, *Macaca mulatta*, *Macaca fascicularis*), which often require complex handling and extensive preparations (eg, intubation for anesthetized MRI). Like rodents, marmosets have reduced biosafety concerns (Biosafety Level 1; they do not carry the herpes B virus) compared with macaques (Biosafety Level 2); this designation simplifies housing, husbandry, and transportation to the MRI suite.[24]

Likely concomitant with their elaborated frontal cortex,[25] marmosets have a rich behavioral repertoire as well as specialized circuitry for face processing and vocalization that parallels Old World primates, including humans.[26,27] These features are uniquely paired with a lissencephalic (ie, smooth) cortex, as in rodents. This flat cortical surface lends itself well to invasive methodologies that would otherwise either cause damage by crossing through a gyrus (eg, electrode implantation, injections) or benefit from a less complex surface morphology (eg, calcium imaging). Such techniques are well suited for combination with MRI, opening up many possibilities for multimodal imaging in marmosets. With the advent of transgenic modification techniques,[28–30] marmosets have gained significant traction as a powerful complement to Old World macaques and are poised to make major contributions to preclinical investigations of the pathophysiology of human brain disorders as well as more basic mechanistic explorations of the brain.

Albeit at a nascent stage compared with macaques and rodents, the number of MRI publications in marmosets has grown markedly in recent years (Figure 1), with several groups already having contributed openly available resources, such as MRI-based atlases and 3-dimensional (3D) printable hardware designs[31–39] as an impetus to accelerate progress in the field of marmoset MRI. Indeed, these strategic advances have been leveraged to inform neuroanatomical and functional topologies in marmosets, including the mapping of white matter pathways,[39,40] functional connectivity,[10,41–44] as well as task-based assessments of visual,[45–47] auditory,[48] and tactile processing.[49] Longitudinal designs are a key advantage associated with the non-invasive nature of MRI, allowing for assessment of developmental trajectories[50] and trajectories of disease progression.[51–53] Despite this significant progress, there are still many open questions that are well suited to study with MRI in marmosets (eg, implementation of behavioral tasks, tracking transgenic models). This rings especially true for functional MRI (fMRI) in marmosets, with only a few groups worldwide currently outfitted to perform fMRI in marmosets and fewer than 2 dozen marmoset fMRI publications over the past decade. Here, we discuss practical aspects of implementing MRI and fMRI in marmosets (both under anesthesia and fully awake) and provide an outlook for the growth of marmoset MRI in the future.

Marmoset Imaging Across MRI Platforms

While about the size of a rat (at approximately 350–550 g), the marmoset brain can be imaged using specialized small-animal MRI scanners typically employed for rodent imaging: those with approximately 15- to 30-cm bores used to images animals <500 g. Outfitted at high–magnetic-field strengths (eg, 7–11.7 Tesla) and often with custom gradient and radiofrequency (RF) receive coils, these systems allow for superior signal-to-noise ratio and resolution over clinical-type MRI platforms designed to image the human brain. Although possible, implementation of small-bore marmoset MRI is not trivial due to the technical challenges associated with developing specialized imaging hardware.[34,37,54–56] Commercially available RF coils designed for rodents are often not optimized for the significantly larger marmoset head and brain, especially for accelerated echo-planar imaging sequences requiring multi-channel receive arrays (eg, fMRI, diffusion tensor imaging, arterial spin labeling). To that end, the recent design of geometrically optimized, phased-array receive coils by several

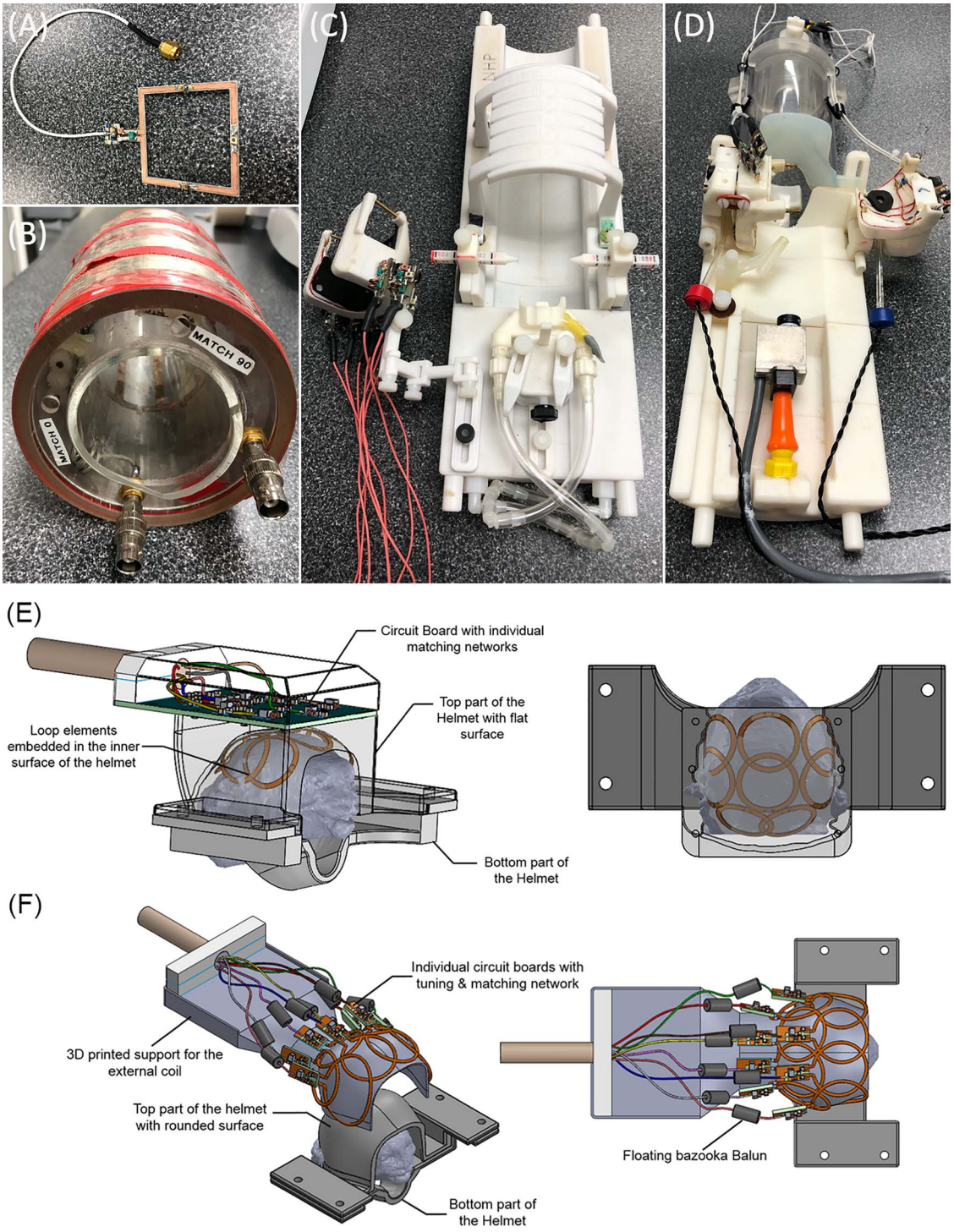

Figure 2: Radiofrequency coils used to image marmosets. (A) A surface coil, which allows for the flexibility of imaging across the marmoset body. (B) A commercially available volume coil, which also offers the flexibility of imaging across the marmoset body. Both (A) and (B) are less well suited for accelerated sequences (eg, fMRI). For this, custom-fitted phased array coils, such as the one shown in (C), which allows for imaging marmosets in stereotactic position under anesthesia, and (D-F), which are designed for imaging marmosets fully awake, are better suited. Panels (E) and (F) show the diagrams of an 8-element phased array coil embedded (E) or external (F) to the restraining helmet.

research groups[55,57] has allowed for major inroads into imaging marmoset cohorts across different sequence types. Such designs for horizontal-bore scanners (Figure 2) are particularly useful for functional imaging studies as they allow for the presentation of visual stimuli to the marmoset in the sphinx position.

Many anatomically focused pulse sequences (eg, T1, T2, proton density-weighted sequences), however, can be more readily achieved with small animal magnets using commercially available coils. For example, surface receive-only RF coils—those with 1 or more elements that are placed close to the surface

(Figure 2A)—or volumetric coils surrounding the subject (often in cylindrical housings; Figure 2B) allow for broad applicability, including body imaging. Indeed, such coils have been used to track changes in brain morphology as a function of motor skill acquisition,[58] localizing function related to vocalization,[59] and acquiring high-quality ex vivo data.[31] As such, many experiments are still possible without the use of geometrically optimized or contoured coils, with standard surface/volume coils often an excellent option for presurgical mapping, diagnostics, and ex vivo sequences. Across all MRI systems, systemic administration (or even local injections) of contrast agents such as manganese can be used to boost the contrast of specific proton relaxivities,[60,61] thus improving the acquired MR signal.

Marmoset imaging is also feasible in large-bore, clinical-type MRI systems, such as those typically employed for human imaging (eg, 3 Tesla). Such systems can be a sensible option for clinical and research facilities not equipped with specialized small-animal MRI hardware, which requires significant investment. Although the lower field strength, gradient power, and sensitivity of receive coils can hamper the signal quality and resolution for some sequences, most clinical MRI systems are fully capable of acquiring high-quality structural images in marmosets. In fact, smaller receive-only RF coils, such as those designed for imaging a human wrist or knee, can be useful for structural or diagnostic imaging in the marmoset in a clinical MRI system.[62] Indeed, such systems have allowed for informative assessments of stroke.[63] In addition to more widespread availability in clinical and research environments, translational studies comparing human and marmoset MR images may benefit from the similarity of relaxivities and contrast parameters by implementing the same main magnetic field strength (B_0) in both species. Many canonical MRI sequences used in humans have been adapted to accommodate the smaller marmoset brain, allowing for comparably short scan times.[62] Another advantage of these larger-bore systems is that marmosets can be imaged in the upright position that is often employed for electrophysiology studies,[64] opening up many possibilities for behavioral or social designs (eg, multiple marmosets interacting) while also allowing for better coil positioning around the back of the head compared with the sphinx position.[38] MRI-compatible, upright-chair systems equipped with custom phased array coils can be purchased commercially (Rogue Research Inc./Takashima Seisakusho Co., LTD) currently for 3 and 7 Tesla Siemens MRI systems.

Apart from adapting MRI hardware and sequences for marmosets, a major challenge for acquiring high-quality MRI in marmosets is minimizing head motion; with spatial encoding central to most MRI sequences, head motion has a deleterious effect on image quality (eg, mid-TR movement, dynamic changes in the local B_0 field). As such, it is imperative to keep the subject as motionless as possible. As animals that use head movements as a primary means for visual orienting, marmosets are intrinsically not compliant in this regard, and thus it is necessary to intervene with anesthetic regimes that allow for minimization of head movement and also limit stress to the animal. Another option is via mechanical head fixation, which also circumvents the deleterious effects of anesthesia on neural activity and neurovascular coupling[49] but requires training and acclimation procedures. These topics have been the area of intense examination in research in recent years—we discuss the progress of these options in the following sections.

MRI Under Anesthesia

MRI of marmosets often requires the use of anesthetic agents to avoid the effects of motion, physiological stress, and training requirements. Anesthetic regimes, along with analgesics and close physiological monitoring, allow for MRI of marmosets in stereotactic devices, which aid in reproducible surgical guidance and also limit motion during MRI.[37,65] Multiple effective anesthetic regimes have been vetted in marmoset cohorts;[65–69] choosing the appropriate protocol depends not only on the length of the experiment but also on the question of interest. Terminal experiments, for example, may follow a different protocol (eg, urethane) than longitudinal experiments (eg, propofol, isoflurane) that necessitate a full recovery and thus must limit toxicity or excessive suppression of autonomic function. The depth of anesthesia may also vary depending on the sequence of interest, with structural sequences (eg, diffusion imaging) allowing for higher doses of anesthesia than studies focused on brain function (eg, resting-state fMRI). It is worth noting that although anesthesia does decrease animal motion, autonomic processes such as breathing have been shown to produce a non-trivial amount of head motion that can have deleterious effects on the resultant images if not rigidly head fixed (eg, via a stereotaxic device).[37]

Anesthetics, Induction, and Preparation

Among the available anesthetic regimes for maintained insentience (eg, sevoflurane, halothane, propofol; see Silva et al[66] for detailed review), isoflurane has been the most widely used for marmoset MRI, particularly for fMRI studies. As an inhalant anesthetic, isoflurane can be delivered via a mask (Johnston et al[64] for 3D printable design), thus avoiding the need for endotracheal intubation or intravenous catheterization; intubation procedures in marmosets can be difficult and risk-prone compared with macaques. Intravenous catheterization, however, may be otherwise necessary for physiological monitoring (eg, arterial blood gasses) or emergency recovery (eg, delivery of epinephrine). Isoflurane is also relatively easy to control in response to changes in physiological stability, supports a relatively quick recovery (usually within approximately 30 minutes), and is safe for repeated use. That being said, the use of isoflurane is not without caveats—we have recently demonstrated that isoflurane can result in systematic reductions in blood oxygen level-dependent signal and thus obfuscate the full extent of functional connectivity profiles in marmosets.[70] Similar effects have been observed when using propofol in marmosets,[49] with the effects of either agent being dose dependent. With isoflurane having only limited analgesic effects, additional analgesic medications (eg, nonsteroidal anti-inflammatory drugs such as meloxicam or opioids such as buprenorphine)[68] may be needed, especially if stereotactic devices with ear bars are used. Coating the tips of the ear bars with topical analgesics such as xylocaine jelly is also recommended.

Initial sedation and induction can be achieved via intramuscular injection (eg, 20 mg/kg ketamine hydrochloride) or by way of a high initial bolus of halogenated anesthesia (eg, isoflurane, sevoflurane) administered through an induction chamber. Both methods serve to immobilize the marmoset during transition and preparation for maintained anesthesia, whether it involves intubation, fitting of a mask for inhalation, or catheterization for intravenous perfusion. For functional imaging studies using inhalant anesthetics, it may be of use to induce anesthesia with the same agent used for maintenance, thus reducing combinatory effects associated with using a separate drug for induction (eg, ketamine + isoflurane). When using an anesthesia mask, it is particularly important to assure that the airway is clear of salvation, secretions, or other obstructions prior to moving the animal into the MRI. A single dose of atropine sulfate (0.5 mg/kg) 15 to

Table 1 Typical anesthetized marmoset physiological monitoring parameters under anesthesia.

Measure	Range	Unit
Rectal temperature	38–39.5	°C
Mean arterial blood pressure	100–110	mmHg
Pulse oximetry	90–100	%
Heart rate	120–300	BPM
End-tidal CO_2	35–45	mmHg
Respiratory pressure	8–12	cm H_2O
Respiration rate	18–40	BPM

30 minutes prior to induction can help ameliorate fluid blockage of the airway. Prior to imaging, blood glucose can be measured to assess the risk of hypoglycemia, with normal resting rates ranging from 6.9 to 14.3 mmol/L and fasted rates ranging from 5.3 to 5.8 mmol/L; the level can be increased by applying a glucose source to the oral mucosa (eg, granulated sugar and water or honey).

As part of the preparation procedure, physiological monitoring equipment should be affixed to the animal and monitoring started as quickly as it is feasible to assure physiological stability in response to anesthesia. These parameters should be continuously monitored throughout the scanning period, and compensatory mechanisms should be in place if the values exceed the expected range (see Table 1 for normal values; see also[71]). With anesthetic agents such as propofol associated with respiratory depression,[72] it is critical that the animal can be quickly removed from the magnet. This, however, is often not practically achievable with the MRI hardware (eg, coil plugs) and physiological monitoring equipment in place—as such, it may be necessary to intubate the animal to control breathing when using propofol. Monitoring for adequate respiratory function can be achieved via capnography or pulse oximetry, with the former being more readily achieved with the animal intubated; with anesthesia masks, even a small amount of saliva build-up may make mask-based readings impractical. If the end-tidal CO_2 signal is detected outside of the magnet room, the sampling line length to reach the animal inside of the magnet bore should be considered. Pulse oximetry can be more readily implemented with MR-compatible sensors, such as those designed for neonatal applications. Hair removal and placement on the hind paw (with more measurable skin surface than the forepaw) both aid in the reliability of the pulse oximetry signal. Marmosets with darker paw pigment may prove more difficult for reliable readings.

Note that during fMRI sequences, altering the amount of anesthesia may modulate the robustness of the blood oxygen level–dependent signal;[49,70] as such, these changes should be carefully weighed against the effect of the sequence of interest. Apart from movement, compensatory modulation of the anesthetic level does not generally impact non-functional sequences. Because anesthesia affects the regulation of body temperature, countermeasures should be in place to keep the animal warm in MRI environments that requisitely operate at a low temperature (with MRI electronic components adversely affected by heat). Heated water circulation blankets work well for this in combination with insulation (eg, blankets). Simple solutions, such as fabric sacs filled with household rice, can be heated in a microwave oven and placed next to the animal to maintain body temperature. It is worth noting that the sparsely haired belly of the marmoset is more susceptible to burns than other areas of the body if such implements are overheated. Note that all of the monitoring devices, especially those that are electrically powered, should be tested prior to use to assure that these devices do not induce noise or otherwise impact the quality of the MRI signal. Waveguides or other RF shielding can be employed to reduce unwanted effects.

Fully Awake MRI

Given the aforementioned confounds of anesthesia on brain activation, particularly with isoflurane[70] and propofol,[49] fMRI in marmosets is ideally collected with the animal unencumbered by anesthetic agents. The other obvious benefit of collecting fMRI data in awake marmosets is that task-based designs can be employed. With MRI being the only technique that can rapidly image whole-brain functional topologies in vivo, task-based fMRI in marmosets holds tremendous potential for gaining insight into the neural correlates of behavior in this species. Acquiring MRI with a fully awake marmoset is not a trivial task, however, and requires training and acclimation to the MRI environment as well as the animal being head fixed to mitigate motion. A great deal of progress has been made in recent years to allow for head fixation via non-invasive helmets and also via invasive chamber implantation. An overview of these developments is discussed in turn.

Training and Preparation

Detailed training procedures for preparing a marmoset for awake MRI are described in.[71] Generally, these procedures follow the same timeline but may require more time to acclimate the marmosets to a non-invasive restraint system or, alternatively, need to be planned in accordance with the recovery from surgical implantation of a head fixation device. Generally, a marmoset can be trained for awake MRI in as little as a few weeks, but advancements to the subsequent training step should be based on the animal's behavior (see behavioral rating scale in [71]). During the first phase, the marmoset can be acclimatized to the body restraint only (ie, not head restrained) for increasingly long periods of time, starting at 15 minutes and progressing up to an hour in the course of a week. The marmoset should be rewarded (eg, banana pudding, mini-marshmallows) at the start and end of the training session. During the second phase, the marmoset is inserted into a mock MRI tube (ie, the same diameter as the scanner bore being used) while being restrained as described in phase 1. With MRI being an extremely loud technique (eg, 125+ dB for an fMRI sequence at 9.4 Tesla), it is necessary to also acclimate the animal to the periodic sounds of the MRI; this is done by playing recorded versions of the sounds at increasingly loud volumes, and for increasingly long durations. Again, the marmosets should be rewarded at the start and end of the training session. If performance is satisfactory for phase 2, then phase 3 begins. Phase 3 involves the processes of phase 1 (body restraint) and 2 (sounds in the mock MRI), but with the addition of head fixation. This procedure will differ for the hardware system used (described below) but generally should follow the same Behavioral Response Scale described in Silva et al[71] until the marmoset is sufficiently acclimatized to the restraint system and thus is ready for the MRI environment with minimal stress. It is worth noting that at very high field strength (9.4 Tesla),

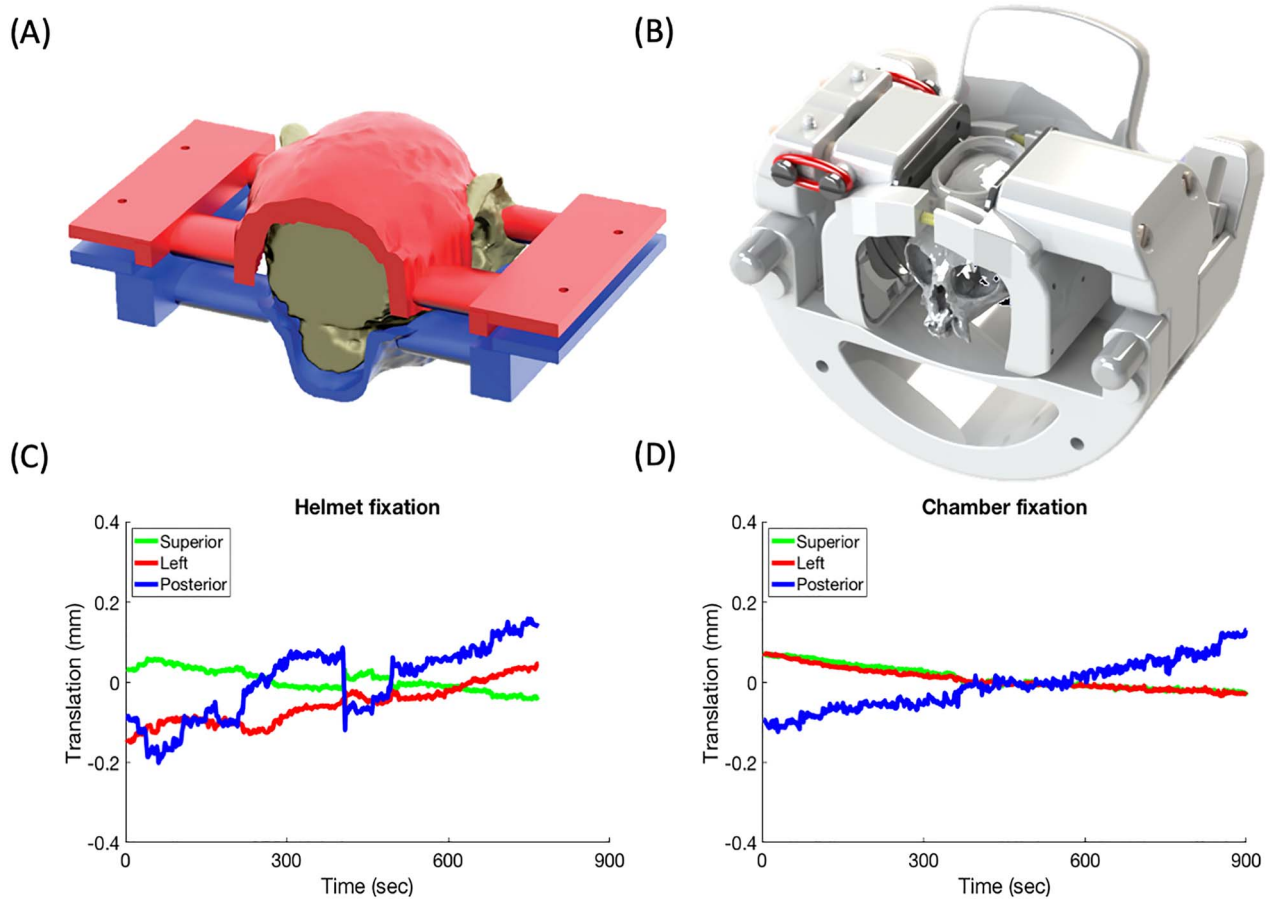

Figure 3: Methods of head fixation for awake marmoset fMRI. (A) A completely non-invasive design that makes use of 3D-printed helmets contoured specifically to each marmoset's head morphology. (B) A chamber-based fixation system in which a 3D-printed head chamber is surgically implanted, then affixed within a clamping system. (C) and (D) head motion (translation) for each respective design.

we have also observed strong visual nystagmus (sometimes resulting in nausea) on the first few MRI sessions. Although this generally seems to adapt within approximately 30 minutes of being within the magnet, we have found that providing some visual stimuli on which the marmoset can fixate helps ameliorate this effect more quickly.

Hardware Developments for Awake MRI

Several options have been shown to be effective for head fixation during awake marmoset fMRI.[38,49,55,73] Here, we discuss the methods developed by our respective laboratories: (1) non-invasive, custom 3D-printed helmets (Figure 3A), and (2) surgically implanted chambers (Figure 3B). Both methods have proven to be highly stable solutions. The first option is customized to the morphology to each marmoset head, and the second option is based on a one-size-fits-all chamber system for adult marmosets (publicly available for download; https://gin.g-node.org/everling_lab_marmosets/awake_marmoset_fMRI_hardware). Both of these systems leverage 3D printing; many commercially available printers are designed to print plastics that are MRI compatible and very low cost when considered against the cost of machining parts.[74] Aside from the cost, the other main benefit of in-house 3D printing is that customizations to the animal bed, coil, or extensions (eg, tactile stimulator, camera attachment) can be quickly built and iteratively developed to fit the needs of the experiment.

Non-invasive Head Restraint. The basic concept of the non-invasive head restraint design is depicted in Figure 3A. For each marmoset, a 3D gradient-echo image is acquired of the entire head and neck.[71] Then, this 3D contour is transferred via computer-aided-design software to a 3D-printed split helmet system; the marmoset is head fixed by tightening the 2 halves together (which are also lined with foam for comfort). As shown in Figure 3C, this design, along with acclimatization, allows for limitation of head movement during fMRI acquisition; because the movements are relatively small (typically <1 voxel), movement-related artifacts can also be removed via nuisance regression of the estimated translation and rotation. This is a well-vetted system, having already been employed to map functional responses to visual,[27,45] auditory,[48] and somatosensory stimuli,[49,75] and also functional network topologies at rest.[10,76,77] A major benefit of this design is that it can be used to non-invasively image marmosets across development by adapting the design as the head grows; this feature is ideal for tracking transgenic models without incurring the additional risk of implantation surgery.

Chamber-based Head Fixation. The original idea for this design (Figure 3B) was to adapt the chamber-based head fixation system used for electrophysiology[38,64] to the MRI environment. Of course, with electrophysiology, the head must be extremely stable (Figure 3D), and we have successfully implemented a surgically implanted chamber in multiple cohorts of marmosets for this purpose.[78–81] The major challenge of implementing this design for the MRI environment was to use an MR compatible cement, as most types of bone cement are specifically designed to be radio-opaque. Through the course of testing different types of cement, we have found that several coats of adhesive resin (All-bond Universal, Bisco, Schaumburg, IL) cured with an ultraviolet dental curing light along with a 2-component dental cement (C & B Cement, Bisco, Schaumburg, IL) produces minimal artifact in MR images. Through the course of numerous surgeries, we have found that the initial coating of the adhesive resin greatly improves holding power, likely due to improved biocompatibility (ie, adhesion of the cement to the resin rather than to the skull directly).

Importantly, given that skull-attached chambers are generally accompanied by magnetic-susceptibility image artifacts (via differences in the magnetic susceptibility between the chamber, adhesive, air, and tissue, as well as the surgical displacement of the skin, fat, and muscle), we recommend mitigating this distortion by filling the chamber with a water-based lubricant gel (MUKO SM321N, Canadian Custom Packaging Company, Toronto, Canada) just before the MRI session begins. This method works by moving large susceptibility mismatches away from the brain, thereby improving B_0 homogeneity in the brain and thus decreasing geometric distortion. Although other easily removable liquids could be used to fill the chamber, the viscous gel allows for application to the brow ridge without dripping into the eyes. Generally, we found that a thin film (of approximately 2–3 mm) of the lubricant gel on the brow ridge was sufficient to ameliorate the associated geometric distortion.

The animal holder was designed to first allow the animals to become acclimatized to the tube design while they were restrained with neck and tail plates (Figure 2D), then for quick and efficient head-fixation through the use of hinged fixation pin assemblies and a retractable clamp (via 2 elastic O-rings). At the front of the assembly is a modular attachment that can be switched between a camera (eg, Model 12 M-i, MRC Systems GmbH, Heidelberg, Germany) and reward tube assembly (for awake behavior) or a separate assembly with a mask for anesthetic delivery (ie, for anesthetized comparisons, or excessively long anatomical imaging). Beyond the customizability of this system, an advantage of this chamber-based system is that it is completely open above the skull, allowing for either within-scanner multimodal imaging (eg, electrophysiology) or the use of complementary techniques outside the scanner in the same animal.

Marmoset MRI Data Processing

Atlases and Template Spaces

To compare results across individual marmosets, it is helpful, and arguably necessary, to register to a common 3D template space. This is a standard practice in human, macaque, and rodent MRI studies.[82–84] For marmosets, a tremendous amount of progress has been made in generating atlases despite the marmoset model only recently gaining popularity for use in MRI (Figure 1). In combination with the paper-based 2-dimensional cytoarchitecture atlas in stereotactic space,[85] a 3D version is now available, carefully registered to an ultra-high resolution structural image.[35] Further, connectivity-based atlases are also registered to the same volumes and surfaces for ease of multimodal comparisons. This atlas is available at https://www.sciencedirect.com/science/article/pii/S1053811917310182?via%3Dihub, along with a more recently published ultra-high-resolution white matter atlas (Figure 5).[39] This work has been developed in tandem with other large consortiums of marmoset researchers aimed at accelerating the progress of marmoset research through the contribution of atlas resources. Impressive efforts from the Brain/MINDS consortium[36,86] and marmosetbrain.org[87,88] have allowed for unprecedented interchangeability between MRI and other methodologies, namely histochemical tracing. These resources are invaluable for validating the comparability of findings across the marmoset scientific literature. For example, they allow comparisons between fMRI-based functional connectivity and cellular-level structural connectivity.[43]

Data Analysis

One of the advantages of MRI is that it yields a similar data structure across different species. As such, for the most part, data analysis procedures can mirror those that have been well established for use in humans, macaques, or rodents[89]—the canonical software packages for image analysis[90,91] have been successfully employed for analysis of marmoset fMRI studies,[41,43,47] with some even including marmoset-specific options and housing the templates described above.[35] Note that data quality, especially fMRI and diffusion tensor imaging data, is contingent not only on the strength and sensitivity of the hardware being used but also on having a well-tuned sequence. For sequences leveraging accelerated acquisitions, the phase-encoding direction can have a substantial impact on the quality of the image as a function of the direction chosen (ie, anterior–posterior, left–right, or superior–inferior) and thus should be carefully examined prior to implementing a study. With the number of channels often being limited on small-animal MRI systems compared with clinical MRIs, accelerated sequences in custom marmoset coils arrays may require adapted strategies compared with MRI of macaques (for technical details regarding the interaction between encoding directions, geometry factor, and concomitant effects on signal quality, see Papoti et al[55]).

In terms of analysis, there are a few special considerations to take when analyzing marmoset MRI data. First, because the eyes are disproportionally large with reference to the brain in marmosets, they can cause non-trivial artifacts depending on the sequence being used (related to the movement of these large, fluid-filled bodies in close proximity to the brain). These effects can often be removed via data-driven noise identification techniques, such as independent component analysis.[92] Second, with the marmoset's lissencephalic cortex and especially thin skull (only 1–2 mm), parameters for brain extraction should be closely examined and often need to be altered from normally acceptable values for human or macaque images or even conducted manually. Third, as is often the case in rodents, physiological artifacts, such as respiration, may be more prominent in marmosets than in humans—if possible, these parameters should be recorded with reference to the timing of the sequence and used as confound regressors in the analysis. As the recording of these parameters can be difficult in fully awake animals, data-driven noise identification and removal techniques may

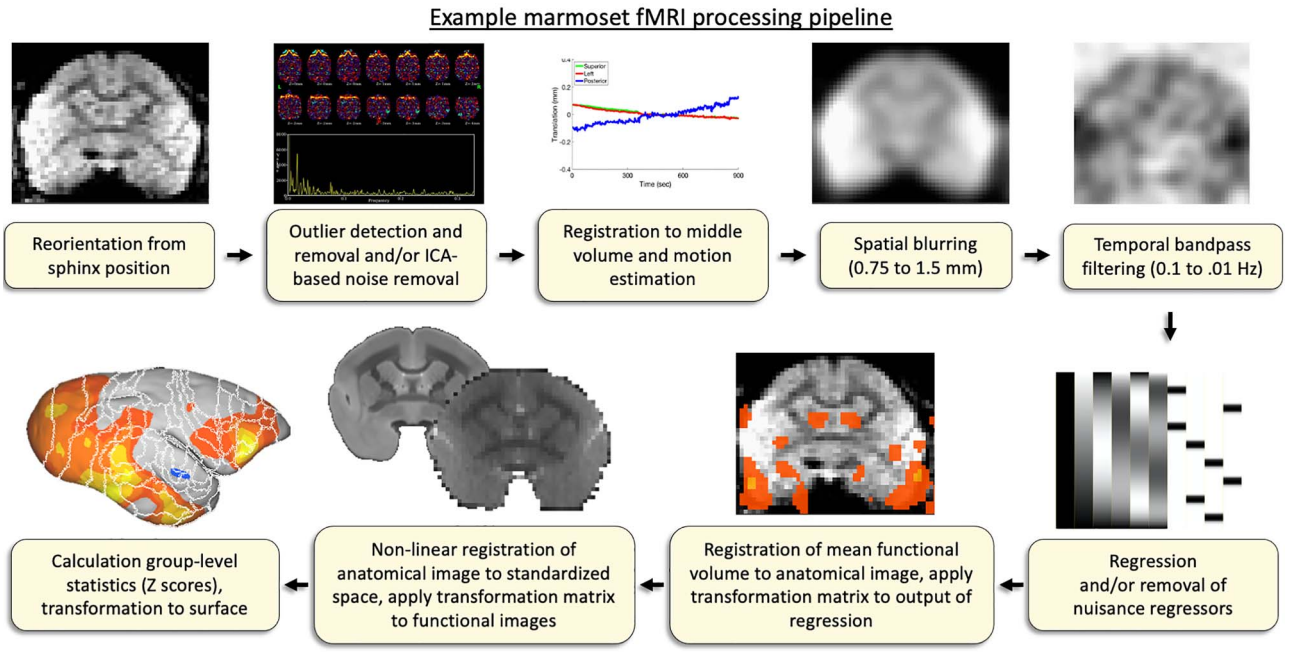

Figure 4: Basic workflow for processing marmoset fMRI data. Note that anatomical images used for registration are manually skull-stripped, including the olfactory bulb.

be of use.[92] We provide a basic example of a marmoset fMRI processing pipeline, as shown in Figure 4.

Outlook and Conclusion

Marmoset MRI is still in its infancy compared with macaque MRI, which has been adopted by many research groups.[3,14] This is partly due to the fairly recent surge in marmoset research, which was largely driven by the creation of the first transgenic marmosets in 2009 by Sasaki and colleagues,[28] whereas macaques have been the standard NHP model for electrophysiological studies for more than 50 years.[93] The goal of this article was to provide an overview of the practical aspects of implementing MRI and fMRI in marmosets with the hope to further promote marmosets as a complementary NHP model for studying brain functions and disorders. We believe that the developments in hardware for data acquisition, analysis pipelines, and brain atlases over the past 7 years have opened up a plethora of possible future applications and directions for marmoset fMRI.

Perhaps the most obvious application is the characterization of global brain network changes in marmoset disease models, ranging from surgical[94,95] and pharmacological approaches[96] to those using genetic modification technologies.[28,30,97] For human brain disorders, fMRI is now the primary technique for investigating large-scale functional connectivity and task-based activation changes.[98] With high-resolution functional acquisitions now possible following recent hardware advances, fMRI is poised to become equally essential for characterizing changes in brain networks in marmoset disease models. The power of this approach is that it affords the application of the same imaging and analysis techniques in both species. This will allow for global phenotyping of disease models with direct comparisons with phenotypic classifications in human patient populations.

In an animal model such as the marmoset, non-invasive fMRI can also be combined with invasive techniques such as optogenetics[99] and chemogenetics[100] that will allow manipulation of the excitatory state of selected neurons. Some of these techniques,[13] as well as more traditional approaches such as electrical microstimulation[15–18] or temporary pharmacological inactivations,[101] have already been successfully employed in fMRI studies in macaque monkeys. Although the combination of these invasive approaches with fMRI is probably more challenging in the smaller marmoset brain—primarily because of magnetic-susceptibility image artifacts by probes or surgical alterations of the skull—they are worth pursuing because they will likely advance our understanding of functional brain networks in primates. Once the technical challenges are overcome, these interventional techniques will also be valuable in probing network changes in disease models.

With regard to non-invasive techniques, another obvious application for MRI and fMRI is longitudinal developmental studies. So far, there is only 1 study, by Sawiak and colleagues,[50] that employed MRI to systematically investigate the growth trajectories of cortical and subcortical regions in marmosets. Consistent with developmental studies in humans,[102,103] the authors found that the prefrontal cortex shows late maturational changes during adolescence. In addition, the authors showed that the prefrontal cortex also has the greatest intraregional variability of growth patterns. This finding is particularly relevant for neuropsychiatric disorders, which typically have their onset during late adolescence and early adulthood.[104] Future developmental studies using resting-state fMRI and potentially also task-based fMRI in marmosets will allow direct comparison of neural network developments shown in humans. Developmental MRI and fMRI studies will also be essential in marmoset models of neuropsychiatric diseases. The clear advantage of the non-invasive fMRI technique for these studies is that the animals do not have to be euthanized at different study time points, which is particularly important for certain transgenic disease models where only a few animals

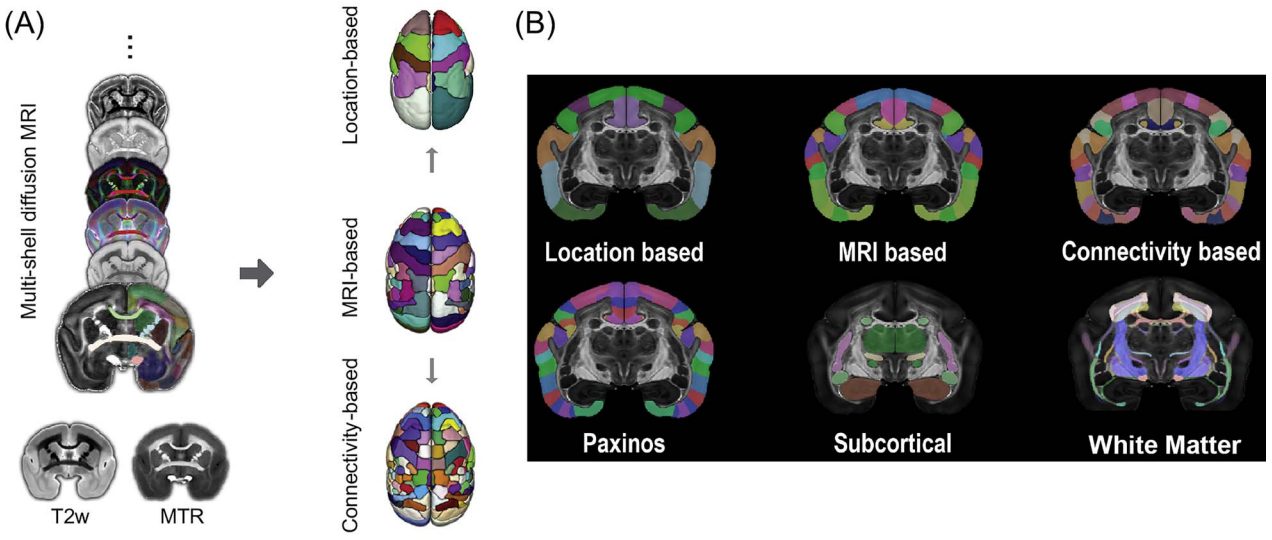

Figure 5: (**A**) The marmoset brain atlas was built from a set of ex-vivo multimodal high-resolution MRI images from the male marmoset brain sample that included multi-shell diffusion MRI, T2w, and magnetization transfer ratio (MTR). Based on the manifold local MRI contrasts, we manually delineated 54 cortical areas and 16 subcortical regions on 1 brain hemisphere. From this original version, we also created a coarser version with 13 larger cortical regions joined together based on their spatial locations, as well as a refined version in which 106 cortical areas were determined by performing a connectivity-based parcellation using diffusion tractography. (**B**) Top row: the marmoset brain parcellation based on the regional location (left), MRI segmentation (middle), and connectivity-based analysis (right). Bottom-row: the marmoset brain parcellation based on the Paxinos atlas (left), subcortical structures (middle), and white-matter fiber pathways (right).

are available. A challenging aspect of developmental studies in marmosets, in particular when they will be conducted in awake animals, is the method of head-fixation; 1 solution may be custom printed 3D helmets, as described above.

Finally, although large strides have been made in the development of RF coils and restrain systems for awake marmoset fMRI at ultra-high fields, a number of brain areas are still difficult to image with current RF coils when animals are in the sphinx position. In particular posterior parts of the primary visual cortex, the cerebellum, brain stem, and thalamus usually have a low signal-to-noise ratio related to the position of the head and neck and the accompanying magnetic susceptibility profile.[37,38] Particularly for fMRI of the cerebellum and brain stem, it might be necessary to develop RF coils and restrain systems for the marmoset in the supine position. Sequence development and tuning may also improve the ability to acquire high-quality laminar fMRI that will allow for layer-specific assessments of activation. As more groups adopt the marmoset as a powerful NHP model, we anticipate that MRI techniques will become an essential tool for studying large scale neural networks in this species.

Acknowledgments

We thank Miranda Bellyou, Cheryl Vander Tuin, Whitney Froese, and Kathrine Faubert for recommendations on animal preparation, anesthesia, and care, and Dr Alex Li for scanning assistance.

Funding

This work was supported by the Canadian Institutes of Health Research (FRN 148365, FRN 353372), a Brain Canada Platform Support Grant, and the Canada First Research Excellence Fund to BrainsCAN. This work was supported in part by the Pennsylvania Department of Health Commonwealth Universal Research Enhancement (C.U.R.E.) Tobacco Appropriation Funds – Phase 18 (SAP 4100083102) to Afonso C. *Silva*.

Potential conflicts of interest. All authors: No reported conflicts.

References

1. Logothetis NK. What we can do and what we cannot do with fMRI. *Nature* 2008; 453(7197):869–878. doi: 10.1038/nature06976.
2. Ogawa S, Lee TM, Kay AR et al. Brain magnetic resonance imaging with contrast dependent on blood oxygenation. *Proc Natl Acad Sci U S A* 1990; 87(24):9868–9872. doi: 10.1073/pnas.87.24.9868.
3. Milham M, Petkov CI, Margulies DS et al. Accelerating the evolution of nonhuman primate neuroimaging. *Neuron* 2020; 105(4):600–603. doi: 10.1016/j.neuron.2019.12.023.
4. Schrago CG, Russo CAM. Timing the origin of new world monkeys. *Mol Biol Evol* 2003; 20(10):1620–1625. doi: 10.1093/molbev/msg172.
5. Schaeffer DJ, Johnston KD, Gilbert KM et al. In vivo manganese tract tracing of frontal eye fields in rhesus macaques with ultra-high field MRI: comparison with DWI tractography. *NeuroImage* 2018; 181(June):211–218. doi: 10.1016/j.neuroimage.2018.06.072.
6. Saleem KS, Pauls JM, Augath M et al. Magnetic resonance imaging of neuronal connections in the macaque monkey. *Neuron* 2002; 34(5):685–700. doi: 10.1016/S0896-6273(02)00718-3.
7. Mars RB, Jbabdi S, Sallet J et al. Diffusion-weighted imaging tractography-based parcellation of the human parietal cortex and comparison with human and macaque resting-state functional connectivity. *J Neurosci* 2011; 31(11):4087–4100. doi: 10.1523/JNEUROSCI.5102-10.2011.
8. Hutchison RM, Leung LS, Mirsattari SM et al. Resting-state networks in the macaque at 7T. *NeuroImage* 2011; 56(3):1546–1555. doi: 10.1016/j.neuroimage.2011.02.063.

9. Hutchison RM, Everling S. Broad intrinsic functional connectivity boundaries of the macaque prefrontal cortex. *NeuroImage* 2014; 88:202–211. doi: 10.1016/j.neuroimage.2013.11.024.
10. Liu C, Yen CCC, Szczupak D et al. Anatomical and functional investigation of the marmoset default mode network. *Nat Commun* 2019; 10(1):1–8. doi: 10.1038/s41467-019-09813-7.
11. Hutchison RM, Everling S. Monkey in the middle: why non-human primates are needed to bridge the gap in resting-state investigations. *Front Neuroanat* 2012; 6(July):1–19. doi: 10.3389/fnana.2012.00029.
12. Shepherd SV, Freiwald WA. Functional networks for social communication in the macaque monkey. *Neuron* 2018; 99(2):413–420.e3. doi: 10.1016/j.neuron.2018.06.027.
13. Gerits A, Farivar R, Rosen BR et al. Optogenetically induced behavioral and functional network changes in primates. *Curr Biol* 2012; 22(18):1722–1726. doi: 10.1016/j.cub.2012.07.023.
14. Milham MP, Ai L, Koo B et al. An open resource for non-human primate imaging. *Neuron* 2018; 100(1):61–74.e2. doi: 10.1016/j.neuron.2018.08.039.
15. Tolias AS, Sultan F, Augath M et al. Mapping cortical activity elicited with electrical microstimulation using fMRI in the macaque. *Neuron* 2005; 18(6):901–911. doi: 10.1016/j.neuron.2005.11.034.
16. Ekstrom LB, Roelfsema PR, Arsenault JT et al. Bottom-up dependent gating of frontal signals in early visual cortex. *Science (80)* 2008; 321(5887):414–417. doi: 10.1126/science.1153276.
17. Field CB, Johnston K, Gati JS et al. Connectivity of the primate superior colliculus mapped by concurrent microstimulation and event-related fMRI. *PLoS One* 2008; 3(12):e3928. doi: 10.1371/journal.pone.0003928.
18. Nikos L. Electrical microstimulation and fMRI. *Front Behav Neurosci* 2009. doi: 10.3389/conf.neuro.08.2009.09.005. Available at: https://pubmed.ncbi.nlm.nih.gov/16364895/.
19. Pawela CP, Biswal BB, Cho YR et al. Resting-state functional connectivity of the rat brain. *Magn Reson Med* 2008; 59(5):1021–1029. doi: 10.1002/mrm.21524.
20. Lu H, Zou Q, Gu H et al. Rat brains also have a default mode network. *Proc Natl Acad Sci U S A* 2012; 109(10):3979–3984. doi: 10.1073/pnas.1200506109.
21. Leergaard TB, Bjaalie JG, Devor A et al. In vivo tracing of major rat brain pathways using manganese-enhanced magnetic resonance imaging and three-dimensional digital atlasing. *NeuroImage* 2003; 20(3):1591–1600. doi: 10.1016/j.neuroimage.2003.07.009.
22. Miller CT, Freiwald WA, Leopold DA et al. Marmosets: a neuroscientific model of human social behavior. *Neuron* 2016; 90(2):219–233. doi: 10.1016/j.neuron.2016.03.018.
23. Silva AC. *Anatomical and funcitonal neuroimaging in awak, behaving marmosets* 2017; 77(3):373–389. doi: 10.1016/j.trsl.2014.08.005.The.
24. Rensing S, Oerke AK. Husbandry and management of new world species. Marmosets and tamarins. *Lab Primate* 2005; 145–162. doi: 10.1016/B978-012080261-6/50010-6. Available at: https://www.ncbi.nlm.nih.gov/pmc/articles/PMC7149791/.
25. Solomon SG, Rosa MGP. A simpler primate brain: the visual system of the marmoset monkey. *Front Neural Circuits* 2014; 8:96. doi: 10.3389/fncir.2014.00096.
26. Kato Y, Gokan H, Oh-Nishi A et al. Vocalizations associated with anxiety and fear in the common marmoset (Callithrix jacchus). *Behav Brain Res* 2014; 275:43–52. doi: 10.1016/j.bbr.2014.08.047.
27. Hung C-C, Yen CC, Ciuchta JL et al. Functional mapping of face-selective regions in the Extrastriate visual cortex of the marmoset. *J Neurosci* 2015; 35(3):1160–1172. doi: 10.1523/JNEUROSCI.2659-14.2015.
28. Sasaki E, Suemizu H, Shimada A et al. Generation of transgenic non-human primates with germline transmission. *Nature* 2009; 459(7246):523–527. doi: 10.1038/nature08090.
29. Park JE, Zhang XF, Choi SH et al. Generation of transgenic marmosets expressing genetically encoded calcium indicators. *Sci Rep* 2016; 6(May):1–12. doi: 10.1038/srep34931.
30. Tomioka I, Nogami N, Nakatani T et al. Generation of transgenic marmosets using a tetracyclin-inducible transgene expression system as a neurodegenerative disease model. *Biol Reprod* 2017; 97(5):772–780. doi: 10.1093/biolre/iox129.
31. Newman JD, Kenkel WM, Aronoff EC et al. A combined histological and MRI brain atlas of the common marmoset monkey, Callithrix jacchus. *Brain Res Rev* 2009; 62(1):1–18. doi: 10.1016/j.brainresrev.2009.09.001.
32. Hikishima K, Quallo MM, Komaki Y et al. Population-averaged standard template brain atlas for the common marmoset (Callithrix jacchus). *NeuroImage* 2011; 54(4):2741–2749. doi: 10.1016/j.neuroimage.2010.10.061.
33. Guy JR, Sati P, Leibovitch E et al. Custom fit 3D-printed brain holders for comparison of histology with MRI in marmosets. *J Neurosci Methods* 2016; 257:55–63. doi: 10.1016/j.jneumeth.2015.09.002.
34. Gilbert KM, Gati JS, Klassen LM et al. A geometrically adjustable receive array for imaging marmoset cohorts. *NeuroImage* 2017; 156:78–86. doi: 10.1016/j.neuroimage.2017.05.013.
35. Liu C, Ye FQ, Yen CCC et al. A digital 3D atlas of the marmoset brain based on multi-modal MRI. *NeuroImage* 2018; 169(July 2017):106–116. doi: 10.1016/j.neuroimage.2017.12.004.
36. Woodward A, Hashikawa T, Maeda M et al. Data descriptor: The brain/MINDS 3D digital marmoset brain atlas. *Sci Data* 2018; 5:1–12. doi: 10.1038/sdata.2018.9.
37. Gilbert KM, Schaeffer DJ, Gati JS et al. Open-source hardware designs for MRI of mice, rats, and marmosets: integrated animal holders and radiofrequency coils. *J Neurosci Methods* 2019; 312(September 2018):65–72. doi: 10.1016/j.jneumeth.2018.11.015.
38. Schaeffer DJ, Gilbert KM, Hori Y et al. Integrated radiofrequency array and animal holder design for minimizing head motion during awake marmoset functional magnetic resonance imaging. *NeuroImage* 2019; 193(January):126–138. doi: 10.1016/j.neuroimage.2019.03.023.
39. Liu C, Ye FQ, Newman JD et al. A resource for the detailed 3D mapping of white matter pathways in the marmoset brain. *Nat Neurosci* 2020; 23(2):271–280. doi: 10.1038/s41593-019-0575-0.
40. Schaeffer DJ, Adam R, Gilbert KM et al. Diffusion-weighted tractography in the common marmoset monkey at 9.4t. *J Neurophysiol* 2017; 118(2):1344–1354. doi: 10.1152/jn.00259.2017.
41. Schaeffer DJ, Gilbert KM, Ghahremani M et al. Intrinsic functional clustering of anterior cingulate cortex in the common marmoset. *NeuroImage* 2019; 186(August 2018):301–307. doi: 10.1016/j.neuroimage.2018.11.005.

42. Schaeffer DJ, Gilbert KM, Gati JS et al. Intrinsic functional boundaries of lateral frontal cortex in the common marmoset monkey. *J Neurosci* 2019; 39(6):1020–1029. doi: 10.1523/JNEUROSCI.2595-18.2018.
43. Hori Y, Schaeffer DJ, Gilbert KM et al. Comparison of resting-state functional connectivity in marmosets with tracer-based cellular connectivity. *NeuroImage* 2020; 204(July 2019):116241. doi: 10.1016/j.neuroimage.2019.116241.
44. Ghahremani M, Hutchison RM, Menon RS et al. Frontoparietal functional connectivity in the common marmoset. *Cereb Cortex* 2016; 1:1–16. doi: 10.1093/cercor/bhw198.
45. Hung CC, Yen CC, Ciuchta JL et al. Functional MRI of visual responses in the awake. *behaving marmoset Neuroimage* 2015; 120:1–11. doi: 10.1016/j.neuroimage.2015.06.090.
46. Schaeffer DJ, Gilbert KM, Hori Y et al. Task-based fMRI of a free-viewing visuo-saccadic network in the marmoset monkey. *NeuroImage* 2019; 202(May):116147. doi: 10.1016/j.neuroimage.2019.116147.
47. Cléry JC, Schaeffer DJ, Hori Y et al. Looming and receding visual networks in awake marmosets investigated with fMRI. *NeuroImage* 2020; 215(April) 116815. doi: 10.1016/j.neuroimage.2020.116815. Available at: https://www.sciencedirect.com/science/article/pii/S1053811920303025.
48. Toarmino CR, Yen CCC, Papoti D et al. Functional magnetic resonance imaging of auditory cortical fields in awake marmosets. *NeuroImage* 2017; 162(April):86–92. doi: 10.1016/j.neuroimage.2017.08.052.
49. Liu JV, Hirano Y, Nascimento GC et al. fMRI in the awake marmoset: somatosensory-evoked responses, functional connectivity, and comparison with propofol anesthesia. *NeuroImage* 2013; 78:186–195. doi: 10.1016/j.neuroimage.2013.03.038.
50. Sawiak SJ, Shiba Y, Oikonomidis L et al. Trajectories and milestones of cortical and subcortical development of the marmoset brain from infancy to adulthood. *Cereb Cortex* 2018; 28(12):4440–4453. doi: 10.1093/cercor/bhy256.
51. Lipsanen A, Kalesnykas G, Pro-Sistiaga P et al. Lack of secondary pathology in the thalamus after focal cerebral ischemia in nonhuman primates. *Exp Neurol* 2013; 248:224–227. doi: 10.1016/j.expneurol.2013.06.016.
52. Absinta M, Sati P, Reich DS. Advanced MRI and staging of multiple sclerosis lesions. *Nat Rev Neurol* 2016; 12(6):358–368. doi: 10.1038/nrneurol.2016.59.
53. Maggi P, Cummings Macri SM, Gaitán MI et al. The formation of inflammatory demyelinated lesions in cerebral white matter. *Ann Neurol* 2014; 76(4):594–608. doi: 10.1002/ana.24242.
54. Papoti D, Yen CC-C, Mackel JB et al. *Awake marmosets at 7T* 2014; 26(11):1395–1402. doi: 10.1002/nbm.2965.An. Available at: https://www.ncbi.nlm.nih.gov/pmc/articles/PMC4200535/.
55. Papoti D, Yen CCC, Hung CC et al. Design and implementation of embedded 8-channel receive-only arrays for whole-brain MRI and fMRI of conscious awake marmosets. *Magn Reson Med* 2017; 78(1):387–398. doi: 10.1002/mrm.26339.
56. Papoti D, Yen CC-C, Mackel JB et al. An embedded four-channel receive-only RF coil array for fMRI experiments of the somatosensory pathway in conscious awake marmosets. *NMR Biomed* 2013; 26(11):1395–1402. doi: 10.1002/nbm.2965.
57. Gilbert KM, Gati JS, Klassen LM et al. A geometrically adjustable receive array for imaging marmoset cohorts. *NeuroImage* 2017; 156:78–86. doi: 10.1016/j.neuroimage.2017.05.013.
58. Yamazaki Y, Hikishima K, Saiki M et al. Neural changes in the primate brain correlated with the evolution of complex motor skills. *Sci Rep* 2016; 6:1–10. doi: 10.1038/srep31084.
59. Sadagopan S, Temiz-Karayol NZ, Voss HU. High-field functional magnetic resonance imaging of vocalization processing in marmosets. *Sci Rep* 2015; 5:1–15. doi: 10.1038/srep10950.
60. Demain B, Davoust C, Plas B et al. Corticospinal tract tracing in the marmoset with a clinical whole-body 3T scanner using manganese-enhanced MRI. *PLoS One* 2015; 10(9):1–14. doi: 10.1371/journal.pone.0138308.
61. Helms G, Schlumbohm C, Garea-Rodriguez E et al. Pharmacokinetics of the MRI contrast agent gadobutrol in common marmoset monkeys (Callithrix jacchus). *J Med Primatol* 2016; 45(6):290–296. doi: 10.1111/jmp.12227.
62. Helms G, Garea-Rodriguez E, Schlumbohm C et al. Structural and quantitative neuroimaging of the common marmoset monkey using a clinical MRI system. *J Neurosci Methods* 2013; 215(1):121–131. doi: 10.1016/j.jneumeth.2013.02.011.
63. Le Friec A, Desmoulin F, Demain B et al. A reproducible new model of focal ischemic injury in the marmoset monkey: MRI and behavioural follow-up. *Transl Stroke Res* 2021; 12(1):98–111. doi: 10.1007/s12975-020-00804-1.
64. Johnston KD, Barker K, Schaeffer L et al. Methods for chair restraint and training of the common marmoset on oculomotor tasks. *J Neurophysiol* 2018; 119(5):1636–1646. doi: 10.1152/jn.00866.2017.
65. Mundinano I-C, Flecknell PA, Bourne JA. MRI-guided stereotaxic brain surgery in the infant and adult common marmoset. *Nat Protoc* 2016; 11(7):1299–1308. doi: 10.1038/nprot.2016.076.
66. Silva AC, Liu JV, Hirano Y et al. Longitudinal functional magnetic resonance imaging in animal models. *Methods Mol Biol* 2011; 711:281–302. doi: 10.1007/978-1-61737-992-5_14.
67. Ishibashi H. More effective induction of anesthesia using midazolam-butorphanol-ketamine-sevoflurane compared with ketamine-sevoflurane in the common marmoset monkey (Callithrix jacchus). *J Vet Med Sci* 2016; 78(2):317–319. doi: 10.1292/jvms.15-0099.
68. Bakker J, Roubos S, Remarque EJ et al. Effects of buprenorphine, butorphanol or tramadol premedication on anaesthetic induction with alfaxalone in common marmosets (Callithrix jacchus). *Vet Anaesth Analg* 2018; 45(3):309–319. doi: 10.1016/j.vaa.2017.06.009.
69. Konoike N, Miwa M, Ishigami A et al. Hypoxemia after single-shot anesthesia in common marmosets. *J Med Primatol* 2017; 46(3):70–74. doi: 10.1111/jmp.12262.
70. Hori Y, Schaeffer DJ, Gilbert KM et al. Altered resting-state functional connectivity between awake and isoflurane anesthetized marmosets. *Cereb Cortex June* 2020; 30(11):5943–5959. doi: 10.1093/cercor/bhaa168.
71. Silva AC, Liu JV, Hirano Y et al. Longitudinal functional magnetic resonance imaging in animal models. *Methods Mol Biol* 2011; 711:281–302. doi: 10.1007/978-1-61737-992-5.
72. Campagna I, Schwarz A, Keller S et al. Comparison of the effects of propofol or alfaxalone for anaesthesia induction and maintenance on respiration in cats. *Vet Anaesth Analg* 2015; 42(5):484–492. doi: 10.1111/vaa.12231.
73. Meyer JS, Brevard ME, Piper BJ et al. Neural effects of MDMA as determined by functional magnetic resonance imaging and magnetic resonance spectroscopy in awake

marmoset monkeys. *Ann N Y Acad Sci* 2006; 1074:365–376. doi: 10.1196/annals.1369.036.
74. Herrmann K-H, Gärtner C, Güllmar D et al. 3D printing of MRI compatible components: why every MRI research group should have a low-budget 3D printer. *Med Eng Phys* 2014; 36(10):1373–1380. doi: 10.1016/j.medengphy.2014.06.008.
75. Hirano Y, Yen CC, Liu JV et al. Investigation of the BOLD and CBV fMRI responses to somatosensory stimulation in awake marmosets (Callithrix jacchus). *NMR Biomed* 2018; 31(3):1–11. doi: 10.1002/nbm.3864.
76. Belcher AM, Yen CC-C, Notardonato L et al. Functional connectivity hubs and networks in the awake marmoset brain. *Front Integr Neurosci* 2016; 10:9. doi: 10.3389/fnint.2016.00009.
77. Belcher AM, Yen CC, Stepp H et al. Large-scale brain networks in the awake, truly resting marmoset monkey. *J Neurosci* 2013; 33(42):16796–16804. doi: 10.1523/JNEUROSCI.3146-13.2013.
78. Selvanayagam J, Johnston KD, Schaeffer DJ et al. Functional localization of the frontal eye fields in the common marmoset using microstimulation. *J Neurosci* 2019; 39(46):9197–9206. doi: 10.1523/JNEUROSCI.1786-19.2019.
79. Johnston K, Ma L, Schaeffer L et al. *Alpha-oscillations modulate preparatory activity in marmoset area 8Ad Alpha-oscillations modulate preparatory activity in marmoset area*; 2019. Available at: https://pubmed.ncbi.nlm.nih.gov/30651331/.
80. Ghahremani M, Johnston KD, Ma L et al. Electrical microstimulation evokes saccades in posterior parietal cortex of common marmosets. *bioRxiv* January 2019; 122(4):1765–1776. doi: 10.1101/693580.
81. Ma L, Selvanayagam J, Ghahremani M et al. Single-unit activity in marmoset posterior parietal cortex in a gap saccade task. *J Neurophysiol* 2020; 123(3):896–911. doi: 10.1152/jn.00614.2019.
82. Seidlitz J, Sponheim C, Glen D et al. A population MRI brain template and analysis tools for the macaque. *NeuroImage* 2018; 170:121–131. doi: 10.1016/j.neuroimage.2017.04.063.
83. Barrière DA, Magalhães R, Novais A et al. The SIGMA rat brain templates and atlases for multimodal MRI data analysis and visualization. *Nat Commun* 2019; 10(1):5699. doi: 10.1038/s41467-019-13575-7.
84. Glasser MF, Coalson TS, Robinson EC et al. A multimodal parcellation of human cerebral cortex. *Nature* 2016; 536(7615):171–178. doi: 10.1038/nature18933.
85. Paxinos G, Watson C, Petrides M et al. *The Marmoset Brain in Stereotaxic Coordinates*. London: Academic Press; 2012.
86. Okano H, Sasaki E, Yamamori T et al. Brain/MINDS: a Japanese National Brain Project for marmoset neuroscience. *Neuron* 2016; 92(3):582–590. doi: 10.1016/j.neuron.2016.10.018.
87. Majka P, Bai S, Bakola S et al. Open access resource for cellular-resolution analyses of corticocortical connectivity in the marmoset monkey. *Nat Commun* 2020; 11(1):1133. doi: 10.1038/s41467-020-14858-0.
88. Majka P, Chaplin TA, Yu H-H et al. Towards a comprehensive atlas of cortical connections in a primate brain: mapping tracer injection studies of the common marmoset into a reference digital template. *J Comp Neurol* 2016; 524(11):2161–2181. doi: 10.1002/cne.24023.
89. Van Essen DC, Smith SM, Barch DM et al. The WU-Minn human connectome project: an overview. *NeuroImage* 2013; 80:62–79. doi: 10.1016/j.neuroimage.2013.05.041.
90. Cox RW. AFNI: Software for analysis and visualization of functional magnetic resonance neuroimages. *Comput Biomed Res* 1996; 29(29):162–173. doi: 10.1006/cbmr.1996.0014.
91. Smith SM, Jenkinson M, Woolrich MW et al. Advances in functional and structural MR image analysis and implementation as FSL. *NeuroImage* 2004; 23(SUPPL. 1):208–219. doi: 10.1016/j.neuroimage.2004.07.051.
92. Griffanti L, Douaud G, Bijsterbosch J et al. Hand classification of fMRI ICA noise components. *NeuroImage* 2017; 154(December 2016):188–205. doi: 10.1016/j.neuroimage.2016.12.036.
93. Evarts EV. Pyramidal tract activity associated with a conditioned hand movement in the monkey. *J Neurophysiol* 1966; 29(6):1011–1027. doi: 10.1152/jn.1966.29.6.1011.
94. Goldshmit Y, Bourne J. The role of EphA4 during development and following injury in primate brain. *Brain Inj* 2010. Available at: https://pubmed.ncbi.nlm.nih.gov/20486805/.
95. Virley D, Hadingham SJ, Roberts JC et al. A new primate model of focal stroke: endothelin-1-induced middle cerebral artery occlusion and reperfusion in the common marmoset. *J Cereb Blood Flow Metab* 2004; 24(1):24–41. doi: 10.1097/01.WCB.0000095801.98378.4A.
96. Nakako T, Murai T, Ikejiri M et al. Effects of a dopamine D1 agonist on ketamine-induced spatial working memory dysfunction in common marmosets. *Behav Brain Res* 2013; 249:109–115. doi: 10.1016/j.bbr.2013.04.012.
97. Nagai Y, Tomioka I, Ishibashi H et al. Transgenic monkey model of the polyglutamine diseases recapitulating progressive neurological symptoms and polyglutamine protein inclusions. *J Neurol Sci* 2017; 4(2):ENEURO.0250-16.2017. doi: 10.1016/j.jns.2017.08.215.
98. Chen JJ. Functional MRI of brain physiology in aging and neurodegenerative diseases. *NeuroImage* 2019; 187:209–225. doi: 10.1016/j.neuroimage.2018.05.050.
99. Deisseroth K. Optogenetics: 10 years of microbial opsins in neuroscience. *Nat Neurosci* 2015; 18(9):1213–1225. doi: 10.1038/nn.4091.
100. Roth BL. DREADDs for neuroscientists. *Neuron* 2016; 89(4):683–694. doi: 10.1016/j.neuron.2016.01.040.
101. Wilke M, Kagan I, Andersen RA. Functional imaging reveals rapid reorganization of cortical activity after parietal inactivation in monkeys. *Proc Natl Acad Sci U S A* 2012; 109(21):8274–8279. doi: 10.1073/pnas.1204789109.
102. Shaw P, Kabani NJ, Lerch JP et al. Neurodevelopmental trajectories of the human cerebral cortex. *J Neurosci* 2008; 28(14):3586–3594. doi: 10.1523/JNEUROSCI.5309-07.2008.
103. Casey BJ, Giedd JN, Thomas KM. Structural and functional brain development and its relation to cognitive development. *Biol Psychol* 2000; 54(1-3):241–257. doi: 10.1016/S0301-0511(00)00058-2.
104. Larsen B, Luna B. Adolescence as a neurobiological critical period for the development of higher-order cognition. *Neurosci Biobehav Rev* 2018; 94(11):179–195. doi: 10.1016/j.neubiorev.2018.09.005.